Dalton Transactions

Accepted Manuscript

ROYAL SOCIETY OF CHEMISTRY

www.rsc.org/dalton

Journal Name

RSCPublishing

ARTICLE

Mechanisms and rates of proton transfer to coordinated carboxydithioates: studies on $[Ni(S_2CR)\{PhP(CH_2CH_2PPh_2)_2\}]^+$ (R = Me, Et, Bu^n or Ph)†

Cite this: DOI: 10.1039/x0xx00000x

Received 00th January 2012,
Accepted 00th January 2012

DOI: 10.1039/x0xx00000x

www.rsc.org/

Ahmed Alwaaly,[a,b] William Clegg,[a] Richard A. Henderson*,[a] Michael R. Probert[a] and Paul G. Waddell[a]

The complexes $[Ni(S_2CR)(triphos)]BPh_4$ (R = Me, Et, Bu^n or Ph; triphos = $PhP\{CH_2CH_2PPh_2\}_2$) have been prepared and characterised. X-ray crystallography (for R = Et, Ph, C_6H_4Me-4, C_6H_4OMe-4 and C_6H_4Cl-4) shows that the geometry of the five-coordinate nickel in the cation is best described as distorted trigonal bipyramidal, containing a bidentate carboxydithioate ligand with the two sulfur atoms spanning axial and equatorial sites, the other axial site being occupied by the central phosphorus of triphos. The reactions of $[Ni(S_2CR)(triphos)]^+$ with mixtures of HCl and Cl^- in MeCN to form equilibrium solutions containing $[Ni(SH(S)CR)(triphos)]^{2+}$ have been studied using stopped-flow spectrophotometry. The kinetics show that proton transfer is slower than the diffusion-controlled limit and involves at least two coupled equilibria. The first step involves the rapid association between $[Ni(S_2CR)(triphos)]^+$ and HCl to form the hydrogen-bonded precursor, $\{[Ni(S_2CR)(triphos)]^+ \ldots HCl\}$ (K_1^R) and this is followed by the intramolecular proton transfer (k_2^R) to produce $[Ni(SH(S)CR)(triphos)]^{2+}$. In the reaction of $[Ni(S_2CMe)(triphos)]^+$ the rate law is consistent with the carboxydithioate ligand undergoing chelate ring-opening after protonation. It seems likely that chelate ring-opening occurs for all $[Ni(S_2CR)(triphos)]^+$, but only with $[Ni(S_2CMe)(triphos)]^+$ is the protonation step sufficiently fast that chelate ring-opening is rate-limiting. With all other systems, proton transfer is rate-limiting. DFT calculations indicate that protonation can occur at either sulfur atom, but only protonation at the equatorial sulfur results in chelate ring-opening. The ways in which protonation of either sulfur atom complicates the analyses and interpretation of the kinetics are discussed.

Introduction

Proton transfer is one of the most pervasive reactions in chemistry. Understanding the factors that affect the rates of these reactions and, consequently, how to control the rates of these reactions remain important goals. Of particular interest are the rates of proton transfer to sites coordinated to metals.[1] Whilst there have been numerous studies on proton transfer rates to coordinated oxygen sites, there have been few studies on sulfur sites.[2,3] The factors controlling the rates of proton transfers to coordinated sulfur is of fundamental relevance to the action of certain metalloenzymes (such as nitrogenases and hydrogenases), where protonation of a bound substrate occurs at a metal site ligated by cysteinate ligands.[4]

There have been some comparative studies on the protonation of non-coordinated analogous oxygen and sulfur sites. In general, protonation of oxygen sites are diffusion controlled but protonation of the analogous sulfur sites are generally slower (by up to a factor of *ca* 30–50). It has been suggested that the origin of this difference in rates is a consequence of the hydrogen bonding capabilities of the acid and base reactants. Hydrogen bonding occurs prior to proton transfer and stabilizes the transition state for proton transfer. Since sulfur bases are poorer hydrogen bond acceptors than the analogous oxygen bases (with a similar pK_a), proton transfer to sulfur is slower.

There have been few kinetic studies on the protonation of coordinated thiolates. Previously, we have shown that stopped-flow spectrophotometric studies on protonation of coordinated thiolates in [Ni(thiolate)(triphos)]$^+$ (triphos = PhP{$CH_2CH_2PPh_2$}$_2$) can give information about both the initial hydrogen-bonded intermediate and the subsequent intramolecular transfer of the proton.[5] Furthermore, in a recent study we have shown for the isostructural series [Ni(XPh)(triphos)]$^+$ (X = O, S or Se) that the rates of proton transfer from the weak acid, lutH$^+$ (lut = 2,6-dimethylpyridine; pK_a = 14.1 in MeCN),[6] and deprotonation of the complex conjugate acid by lut, are all slow and essentially independent of the donor atom, X.[7] This behaviour is a consequence of the steric bulk of the triphos ligand which limits the access of the sterically-demanding lutH$^+$ to the donor atom.

In this paper we describe the synthesis, structures and protonation chemistry of the 5-coordinate, trigonal bipyramidal [Ni(S_2CR)(triphos)]$^+$ (R = Me, Et, Bu^n or Ph), which contain the bidentate carboxydithioate ligand. Stopped-flow studies show that the reactions of these complexes with anhydrous HCl in MeCN are equilibrium reactions, and involve slow proton transfer. For R = alkyl, the precursor hydrogen-bonded intermediate is detectable. Furthermore, the effect that Cl$^-$ has on the kinetics of the reaction between HCl and [Ni(S_2CMe)(triphos)]$^+$ indicate that, after protonation, the bidentate carboxydithioic acid undergoes chelate ring-opening to form the monodentate ligand (Fig. 1). It seems likely that such chelate ring-opening operates in the reactions of all [Ni(S_2CR)(triphos)]$^+$ species, but when R = Et, Bu^n or Ph proton transfer is slower than chelate ring-opening.

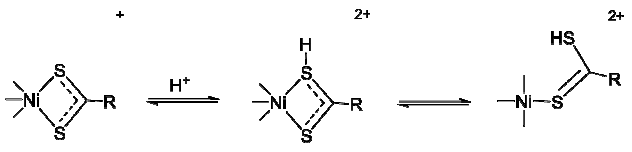

Fig. 1. Protonation and chelate ring-opening of [Ni(S_2CR)(triphos)]$^+$ (triphos omitted for clarity)

Experimental

The following chemicals were purchased from Sigma-Aldrich and used as received without any further purfications: $NiCl_2 \cdot 6H_2O$, benzyltrimethylammonium hydroxide, bis(2-diphenylphosphinoethyl)phenylphosphine = triphos, carbon disulfide, sodium tetraphenylborate, methanol-d_1 and D_2O. CD_3CN was purchased from Goss Scientific and used as received. [NiCl(triphos)]BPh_4 was prepared by the literature method.[8] [NEt_4]Cl was dried *in vacuo* prior to use.

All manipulations in both the synthetic and kinetic aspects of this work were performed under an atmosphere of dinitrogen using Schlenk or syringe techniques, as appropriate.

Synthesis of [NMe_3Bz]S_2CR (Bz = CH_2Ph; R = Me, Et, Bu^n or Ph) All [NMe_3Bz]S_2CR were prepared by the literature method.[9] Manipulations were performed in a fume cupboard. Carbon disulfide (0.78 g, 0.01 mol) in dry THF (20 mL) was slowly added to the appropriate Grignard reagent (10 mL, 0.01 mol) (cooling with a water bath may be necessary), and the mixture was stirred for 1.5 h. About 20 mL of the solvent was removed using a rotatory evaporator, maintaining the temperature below 25 °C. The residue was poured into a mixture of ice (10 g), 10 M hydrochloric acid (5 mL), and hexane (8 mL). The free carboxydithioic acid was extracted with hexane (2 × 5 mL) and the collected organic phases were dried over anhydrous magnesium sulfate. After filtration, [NMe_3Bz]OH (3.5 g of a 40 wt % solution in methanol) was added to the carboxydithioic acid solution. The mixture was then evaporated to dryness *in vacuo*. The deep purple or violet crystals of [NMe_3Bz]S_2CR were washed with cold hexane and dried at room temperature.

Synthesis of [Ni(S_2CR)(triphos)]BPh_4 (R = Me, Et, Bu^n, Ph, C_6H_4X-4) To a suspension of [NiCl(triphos)]BPh_4 (0.5 g; 0.53 mmol) in THF (*ca*. 20 mL) was added [NMe_3Bz]S_2CR (0.25 g; 0.75 mmol). The colour changed rapidly from yellow to dark red, and the mixture became homogeneous. After the solution was stirred for *ca.* 2 h, the solution was filtered and the filtrate was reduce *in vacuo* to *ca*. 10 mL. Addition of an excess of hexane produced a dark red microcrystalline solid. Recrystallization of the complex was achieved by dissolving the solid in the minimum amount of tetrahydrofuran and then adding a large excess of hexane (ca 4–5 × volume of terahydrofuran). Leaving the solution undisturbed at room temperature for 48 h produced red crystals which were dried *in vacuo* (*ca*. 60%). The product was characterized by elemental analysis, ^{1}H NMR and ^{31}P{^{1}H} NMR spectroscopy (Table 1). For R = Et, Ph, C_6H_4Me-4, C_6H_4OMe-4 and C_6H_4Cl-4 the products were also characterized by X-ray crystallography (see Figs. 2 and 3, Tables 2 and 3, and ESI).

Kinetic studies

All kinetic studies were performed using an Applied Photophysics SX.18 MV stopped-flow spectrophotometer, modified to handle air-sensitive solutions, connected to a RISC computer. The temperature was maintained using a Grant LTD6G thermostat tank with combined recirculating pump. The experiments were conducted at 25.0 °C. The wavelength used was λ = 420 nm. All kinetics were studied in MeCN. The MeCN was dried over CaH_2 and distilled immediately prior to use.

Table 1. Elemental analyses and spectroscopic data for $[Ni(S_2CR)(triphos)]BPh_4$ (R = Me, Et, Bu^n or Ph)

Compound	elemental analysis[a] C	H	^1H NMR spectrum	$^{31}P\{^1H\}$ NMR spectrum
$[Ni(S_2CMe)(triphos)]BPh_4$	71.1 (71.8)	6.0 (5.6)	8.45 – 6.75 (m, 45H, *Ph*) 3.50 – 2.23 (br, 8H, CH_2) 1.36 (s, 3H, CH_3)	111.6 (t, J_{PP} = 50 Hz, *PPh*) 47.7 (d, J_{PP} = 50 Hz, PPh_2)
$[Ni(S_2CEt)(triphos)]BPh_4$	71.2 (72.0)	6.0 (5.7)	8.20 – 6.40 (m, 45H, *Ph*) 3.20 – 2.17 (br, 8H, CH_2) 3.73 (q, J_{HH} = 7.3 Hz, 2H, CH_2CH_3) 0.80 (t, J_{HH} = 7.3 Hz, 3H, CH_3)	113.7 (t, J_{PP} = 32 Hz, *PPh*) 52.4 (d, J_{PP} = 32 Hz, PPh_2)
$[Ni(S_2CBu^n)(triphos)]BPh_4$	71.9 (72.4)	6.0 (5.6)	9.10 – 6.79 (m, 45H, *Ph*) 3.40 – 2.50 (br, 8H, CH_2) 3.72 – 3.61 (m, 4H, SCH_2 & CH_2) 1.32 – 1.01 (m, 2H, CH_2) 0.88 (t, J_{HH} = 7.12 Hz, 3H, CH_3)	113.9 (t, J_{PP} = 32 Hz, *PPh*) 51.7 (d, J_{PP} = 32 Hz, PPh_2)
$[Ni(S_2CPh)(triphos)]BPh_4$	71.5 (71.9)	5.9 (5.8)	8.45 – 6.60 (m, 50H, *Ph*) 3.24 – 2.10 (br, 8H, CH_2)	113.0 (t, J_{PP} = 32 Hz, *PPh*) 52.8 (d, J_{PP} = 32 Hz, PPh_2)

footnote: [a] calculated values in parentheses.

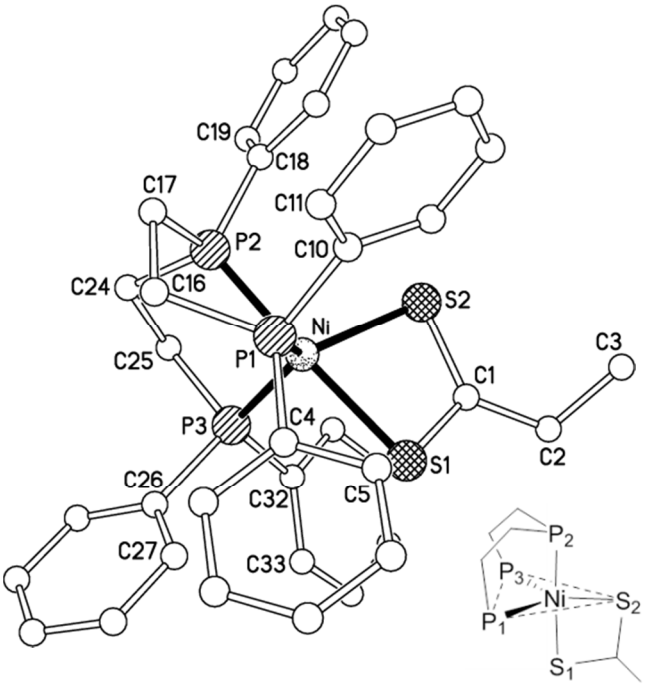

Fig. 2. Structure of the $[Ni(S_2CEt)(triphos)]^+$ cation. H atoms are omitted for clarity; unlabelled atoms follow in sequence from those shown labelled. The inset shows the atom numbering scheme used in Table 2.

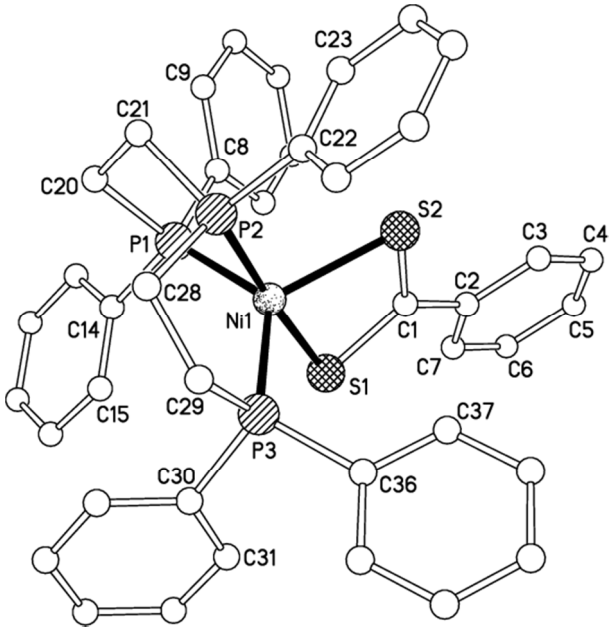

Fig. 3. Structure of the $[Ni(S_2CPh)(triphos)]^+$ cation. H atoms are omitted for clarity.

Table 2. X-ray crystallographic data for two of the $[Ni(S_2CR)(triphos)]BPh_4$ complexes.

complex	R = Et	R = Ph
Formula	$C_{61}H_{58}BNiP_3S_2$	$C_{69}H_{66}BNiOP_3S_2$
M_r / g mol^{-1}	1017.6	1137.8
Crystal system	monoclinic	orthorhombic
Space group	$P2_1/c$	$Pbcn$
a / Å	17.685(4)	38.8301(16)
b / Å	13.749(3)	16.6153(5)
c / Å	22.807(5)	18.1236(5)
β / °	110.150(2)	90
V / Å^3	5206(2)	11692.9(7)
Z	4	8
Reflections measured	66315	52089
Unique reflections, R_{int}	9261, 0.1269	11747, 0.0487
Refined parameters	615	694
R (F, $F^2 > 2\sigma$)	0.0530	0.0486
R_w (F^2, all data)	0.1169	0.1000
Goodness of fit on F^2	1.061	1.070
Max., min. electron density / e Å^{-3}	0.45, −0.39	0.52, −0.38

Table 3. Selected bond lengths and bond angles in $[Ni(S_2CR)(triphos)]^+$ (R = Et or Ph)

complex	R = Et	R = Ph
Bond lengths / Å		
Ni–P1	2.1733(10)	2.2227(7)
Ni–P2	2.1516(11)	2.1484(7)
Ni–P3	2.2174(11)	2.2066(7)
Ni–S1	2.2342(11)	2.2321(7)
Ni–S2	2.3448(10)	2.3179(7)
Bond angles / °		
P1–Ni–P2	85.88(4)	87.70(3)
P2–Ni–P3	87.06(4)	87.39(3)
P1–Ni–P3	131.15(4)	130.66(3)
S1–Ni–S2	75.60(4)	76.16(2)
P1–Ni–S1	95.75(4)	92.70(3)
P1–Ni–S2	125.86(4)	107.41(3)
P2–Ni–S1	176.27(4)	176.60(3)
P2–Ni–S2	100.73(4)	100.50(3)
P3–Ni–S1	94.35(4)	94.90(3)
P3–Ni–S2	102.95(4)	121.76(3)
S1–C–S2	113.7(2)	111.88(15)

The solutions of complex and reactants (HCl and $[NEt_4]Cl$) were prepared under an atmosphere of dinitrogen and transferred to the stopped-flow apparatus using gas-tight, all glass syringes. The kinetics were studied under pseudo-first-order conditions, with HCl and $[NEt_4]Cl$ present in at least a 10-fold excess over the concentration of the complex. Mixtures of HCl and $[NEt_4]Cl$ were prepared from stock solutions of the two reagents. All solutions were used within 1 hour of preparation. Stock solutions of HCl were prepared *in situ*. Thus a solution of HCl (25 mmol dm^{-3}) in 25 mL of CH_3CN was prepared by adding methanol (1.0 mL, 25 mmol) followed by Me_3SiCl (3.175 mL, 25 mmol). Stock solutions of DCl were similarly prepared *in situ* by mixing methanol-d_1 (1.0 mL, 25 mmol) with Me_3SiCl (3.175 mL, 25 mmol) in 25mL of MeCN.

Under all conditions, the stopped-flow absorbance-time trace was an excellent fit to a single exponential, indicating a first-order dependence on the concentration of complex (Fig. 4). The dependences on the concentrations of HCl and Cl^- were determined from analysis of the appropriate graphs as explained in the text in the results and discussion section.

X-ray crystallography

Single crystals of $[Ni(S_2CR)(triphos)]BPh_4 \cdot Sol$ (R = Me, unsolvated; R = Ph, Sol = THF; R = C_6H_4Me-4, Sol = THF or $CHCl_3$; R = C_6H_4OMe-4, Sol = THF; and R = C_6H_4Cl-4, Sol = THF) were examined on various diffractometers at temperatures between 100 and 150 K with either Mo-Kα or synchrotron radiation as detailed in the ESI,. In all cases absorption corrections were applied, based on repeated and symmetry-equivalent reflections, and the structures were solved by direct methods and refined on all unique F^2 values. Disorder was resolved for some of the solvent molecules. Table 2 gives selected crystallographic data for the structures with R = Et and Ph, with selected coordination geometry in Table 3; full information for all six structures is provided in the ESI. The other four structures are all isomorphous, with essentially the same arrangement of cations and anions in the asymmetric unit, the *para* substituents and the solvent molecules occupying equivalent regions in each case, with little variation in the nickel coordination geometry. CCDC references: 1033172–1033177. Programs were standard Agilent Technologies, Bruker and Rigaku control and data processing software, SHELXTL, SHELXL-2014, and OLEX2.[10]

Results and discussion

Synthesis and structures of $[Ni(S_2CR)(triphos)]BPh_4$ All $[Ni(S_2CR)(triphos)]BPh_4$ were prepared by the reactions of $[NMe_3Bz]S_2CR$[9] with $[NiCl(triphos)]BPh_4$ and isolated as dark red crystalline solids. The spectroscopic and analytical data associated with all the complexes are consistent with the formulation (Table 1). The UV-visible spectra of all $[Ni(S_2CR)(triphos)]^+$ in MeCN are very similar broad spectra, absorbing from 350 – 700 nm (R = Et; λ_{max} (shoulder) ~ 510 nm, $\varepsilon = 420$ dm^3 mol^{-1} cm^{-1}). In addition, we have characterised the R = Et, Ph, C_6H_4Me-4, C_6H_4OMe-4 and C_6H_4Cl-4 derivatives by X-ray crystallography. All the crystal structures show discrete cations, anions and, for the aryl derivatives, a molecule of tetrahydrofuran (a chloroform solvate was also characterized for the C_6H_4Me-4 derivative). In the cations, the nickel is 5-coordinate with the coordination sphere made up of the three phosphorus donors of the triphos ligand and the two sulfur atoms of the carboxydithioate ligand. The structures of $[Ni(S_2CEt)(triphos)]^+$ and $[Ni(S_2CPh)(triphos)]^+$ are shown in Figs. 2 and 3, and the structures of the other derivatives are shown in the ESI. The structures of all the cations are best described as trigonal bipyramidal.[11] The trigonal plane comprises the two terminal phosphorus atoms of the triphos ligand and one sulfur from the carboxydithioate ligand. The axial positions of the trigonal bipyramid are occupied by the central phosphorus of the triphos ligand and the other sulfur of the carboxydithioate ligand. Selected bond lengths and bond angles associated with the nickel and its ligands are presented in Table 3 and the ESI.

Previously, we have described the X-ray crystal structure of $[Ni(2\text{-}Spy)(triphos)]BPh_4$ (2-Spy = 2-pyridinethiolate), in which the nickel is also five-coordinate and the 2-Spy ligand is bidentate.[12] The structures of $[Ni(S_2CR)(triphos)]^+$ and $[Ni(2\text{-}Spy)(triphos)]^+$ are very similar. Thus, in $[Ni(2\text{-}Spy)(triphos)]^+$ the structure is also best described as a distorted trigonal bipyramid. Furthermore, the trigonal plane of $[Ni(2\text{-}Spy)(triphos)]^+$ also comprises the two terminal phosphorus atoms (P_{t1}, P_{t2}; subscript t = terminal) of the triphos ligand {Ni–P_{t1} = 2.1637(9) Å, Ni–P_{t2} = 2.1966(9) Å} with the remaining position occupied by the nitrogen of the 2-Spy ligand {Ni–N = 2.164(2) Å, P_{t1}–Ni–P_{t2} = 146.34(3)°, P_{t1}–Ni–N = 119.08(7)°, P_{t2}–Ni–N = 94.11(7)°}. Finally, the two axial positions are occupied by the central phosphorus (P_c) of the triphos ligand and the sulfur of the 2-Spy ligand {Ni–S = 2.2644(8) Å, Ni–P_c = 2.1310(8) Å; P_{t1}–Ni–S = 92.08(3)°; P_{t2}–Ni–S = 93.93(3)°; N–Ni–S = 70.81(6)°; P_{t1}–Ni–P_c = 87.08(3)°, P_{t2}–Ni–P_c = 87.08(3)°, N–Ni–P_c = 109.12(7)°, P_c–Ni–S = 178.98(4)°}.

Kinetics and mechanism.
The kinetics of the reactions of $[Ni(S_2CR)(triphos)]^+$ (R = Me, Et, Bu^n or Ph) with mixtures of HCl and Cl$^-$ {equation (1)} were studied under pseudo-first-order conditions ([HCl]/[Ni] ≥ 10) in MeCN using stopped-flow spectrophotometry. When monitored at a single wavelength, the absorbance-time traces are excellent fits to a single exponential consistent with the reaction exhibiting a first-order dependence on the concentration of $[Ni(S_2CR)(triphos)]^+$ (Fig. 4). The traces exhibit behaviour characteristic of an equilibrium reaction {equation (1)}. Thus, increasing the concentration of HCl (at a constant concentration of Cl$^-$) results in a larger absorbance change and final absorbance, while increasing the concentration of Cl$^-$ (at a constant concentration of HCl) results in a smaller absorbance change and final absorbance (see ESI).

$$[Ni(S_2CR)(triphos)]^+ + HCl \rightleftharpoons [Ni(HS_2CR)(triphos)]^{2+} + Cl^- \quad (1)$$

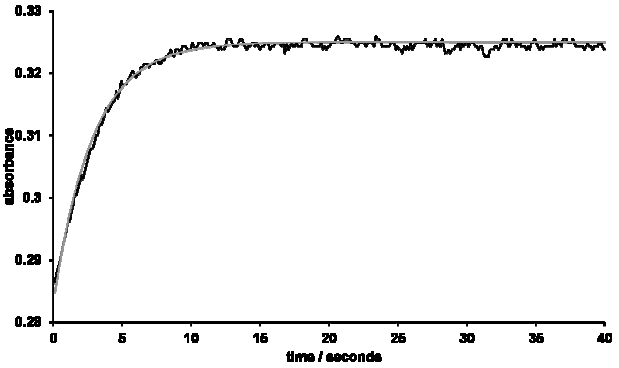

Fig. 4. Stopped-flow absorbance-time curve for the reaction of $[Ni(S_2CEt)(triphos)]$+ (0.5 mmol dm^{-3}) with HCl (40 mmol dm^{-3}) in MeCN at 25.0 °C (λ = 420 nm). The experimental trace is shown in black and the exponential curve fit is shown in grey. The curve fit is defined by the equation $A_t = 0.325 - 0.042\exp(-0.35t)$.

In the discussion below, we will first present the kinetic results of the studies of the R = Me, Et or Bu^n complexes with HCl alone and then report the different effects that introducing Cl$^-$ has on the kinetics of these systems. We will then discuss the possible mechanisms consistent with the kinetics of these systems and, finally, present the kinetics of the R = Ph complex with mixtures of HCl and Cl$^-$ to show that the kinetics of this system are also consistent with the proposed mechanism.

Reaction between $[Ni(S_2CR)(triphos)]$ (R = Me, Et or Bu^n) and HCl. The kinetics of the reactions of $[Ni(S_2CR)(triphos)]^+$ (R = Me, Et or Bu^n) with anhydrous HCl (in the absence of $[NEt_4]Cl$) exhibit a complicated dependence on the concentration of HCl, as shown in Fig. 5. At low concentrations of HCl the reaction exhibits a first-order dependence on [HCl] but at high concentrations of HCl the rate of the reaction is independent of [HCl]. The data were analysed by the usual plot of $1/k_{obs}$ versus 1/[HCl] which is a straight line and allows derivation of the experimental rate law shown in equation (2).[13] When R = Me: $a = 4.69 \times 10^3$ dm^3 mol^{-1} s^{-1}, $b = 67.0$ dm^3 mol^{-1}; R = Et: $a = 39.5$ dm^3 mol^{-1} s^{-1}, $b = 84.0$ dm^3 mol^{-1}; R = Bu^n: $a = 19.9$ dm^3 mol^{-1} s^{-1}, $b = 71.0$ dm^3 mol^{-1}.

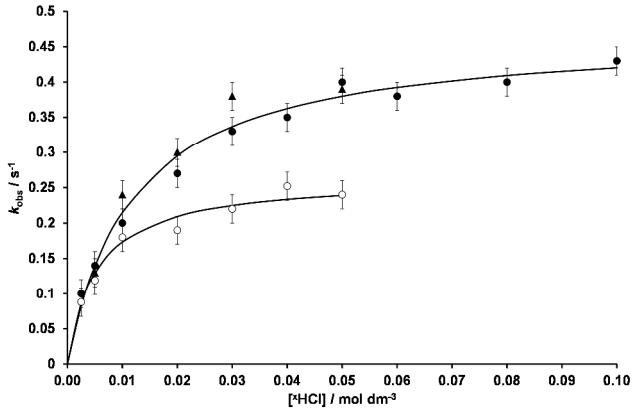

Fig. 5. Kinetic data for the reaction of $[Ni(S_2CEt)(triphos)]^+$ ([Ni] = 0.5 mmol dm^{-3}) with HCl (● and ▲) or DCl (○) in MeCN at 25.0 °C. Curve fits to the data are those defined by Equation (2) and the parameters presented in the text. The different types of filled symbols show the results in different experiments and give an indication of the scatter of the data. The error bars correspond to 10% errors.

$$\text{Rate} = \frac{a[\text{HCl}][\text{Ni}(S_2\text{CR})(\text{triphos})^+]}{1 + b[\text{HCl}]} \qquad (2)$$

Effect of Cl^- on the reaction between $[Ni(S_2CR)(triphos)]$ (R = Me, Et or Bu^n) and HCl. In further kinetic studies, the effect that Cl^- (addition of $[NEt_4]Cl$) has on the rates of the reactions with HCl was investigated. The effect that Cl^- has on the rate of reaction between anhydrous HCl and $[Ni(S_2CEt)(triphos)]^+$ or $[Ni(S_2CBu^n)(triphos)]^+$ is different to the effect Cl^- has on the reaction between HCl and $[Ni(S_2CMe)(triphos)]^+$. For the reactions of HCl with the R = Et or Bu^n derivatives, addition of Cl^- accelerates the rate, whereas in the reaction with the R = Me derivative, Cl^- inhibits the reaction (see ESI).

In analysing the kinetic data for the reactions involving mixtures of HCl and Cl^-, corrections need to be made to the concentrations of these species because, in MeCN, HCl and Cl^- associate as shown in equation (3) (homoconjugation equilibrium).[14]

$$HCl + Cl^- \underset{}{\overset{K_H}{\rightleftharpoons}} HCl_2^- \qquad (3)$$

An important consequence of this equilibrium reaction is that the concentrations of HCl and Cl^- cannot be changed independently; changing the concentration of one will perturb the concentration of the other. Using the literature value of K_H = 158.5 dm^3 mol^{-1}, the concentrations of free HCl and Cl^- present in the mixtures have been calculated {henceforth designated $[HCl]_e$ and $[Cl^-]_e$}.[9] In the kinetic analysis that follows, it is assumed that HCl_2^- acts as neither acid nor base.

For the reactions of the R = Et or Bu^n derivatives with HCl (in the absence of Cl^-), the dependence on the concentration of acid is described by equation (2). Thus, the observed rate constant (k_{obs}) for the reactions in the presence of Cl^- can be corrected for changes to the rate due to changes in the concentration of HCl using ($k_{obs} - k'^R$), where $k'^R = a[HCl]_e/(1 + b[HCl]_e)$. A plot of ($k_{obs} - k'^R$) versus $[Cl^-]_e$ then describes the effect that Cl^- has on the rate of the reaction. Such a plot is a straight line going through the origin (Fig. 6, top). Analysis of this graph shows that, for the R = Et or Bu^n complexes the rate law is that shown in equation (4). When R = Et: c = 380 dm^3 mol^{-1} s^{-1}; R = Bu^n: c = 74 dm^3 mol^{-1} s^{-1}.

$$\text{Rate} = \left\{\frac{a[\text{HCl}]_e}{1 + b[\text{HCl}]_e} + c[Cl^-]_e\right\}[\text{Ni}(S_2\text{CR})(\text{triphos})^+] \qquad (4)$$

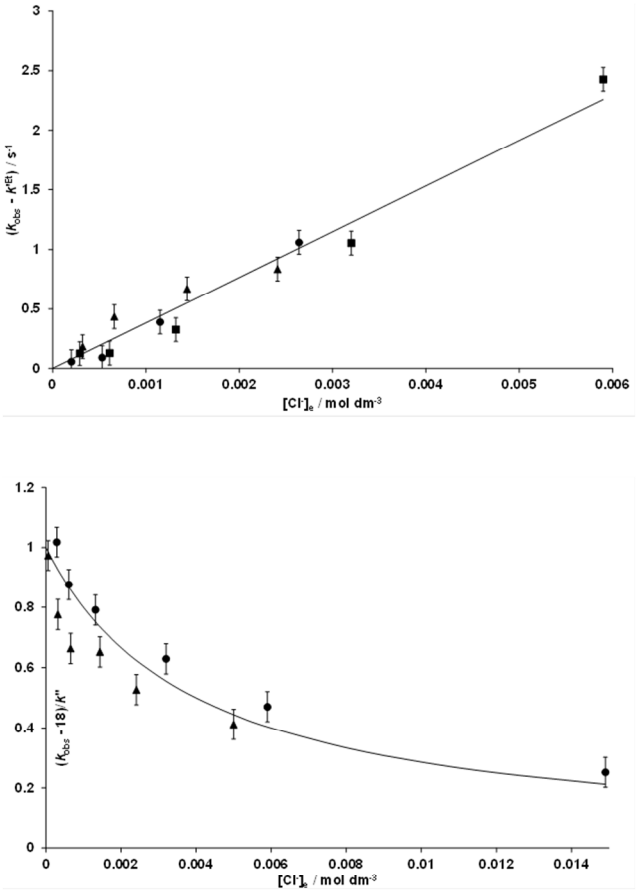

Fig. 6. TOP. Kinetic data for the reaction of $[Ni(S_2CEt)(triphos)]^+$ (0.5 mmol dm^{-3}) with HCl in the presence of Cl^- in MeCN at 25.0 °C. Graph of ($k_{obs} - k'^{Et}$) versus $[Cl^-]_e$ where k'^{Et} and subscript e are explained in the text. Data points correspond to: [HCl] = 25.0 mmol dm^{-3}, [Cl^-] = 1.0–10.0 mmol dm^{-3} (●); [HCl] = 50.0 mmol dm^{-3}, [Cl^-] = 2.5–30.0 mmol dm^{-3} (■); [HCl] = 100.0 mmol dm^{-3}, [Cl^-] = 2.5–30.0 mmol dm^{-3} (▲). Line drawn is that defined by equation (4) and the parameters detailed in the text. BOTTOM. Kinetic data for the reaction of $Ni(S_2CMe)(triphos)]^+$ (0.5 mmol dm^{-3}) with HCl in the presence of Cl^- in MeCN at 25.0 °C. Graph of (k_{obs} – 18)/k'' versus $[Cl^-]_e$ where k' and subscript e are explained in the text. Data points correspond to: [HCl] = 50.0 mmol dm^{-3}, [Cl^-] = 2.5–50.0 mmol dm^{-3} (●); [HCl] = 100.0 mmol dm^{-3}, [Cl^-] = 2.5–50.0 mmol dm^{-3} (▲). Curve drawn is that defined using equation (5) and the parameters detailed in the text. The error bars correspond to 10% errors.

For the reaction of the R = Me complex with mixtures of HCl and Cl^- the analysis of the kinetics is more complicated because addition of Cl^- inhibits the reaction. Initial inspection of the kinetic data (after correcting the concentrations of HCl and Cl^- for the homoconjugation equilibrium but before correcting k_{obs}

for the dependence on the concentration of HCl) showed that: (i) increasing the concentration of Cl^- leads to a decrease in k_{obs} and (ii) at high concentrations of Cl^-, the reaction rate is not zero, but levels off at $k_{obs} \sim 18\ s^{-1}$. To analyse the data, the values of k_{obs} (for the reaction in the presence of Cl^-) were corrected for both the effect of changes to the concentration of HCl, as described by equation (2) and given by $k'' = 4.69 \times 10^3[HCl]_e/(1 + 67.0[HCl]_e)$, and the limiting rate constant at high concentrations of Cl^- ($k_{obs} = 18\ s^{-1}$). Thus, a plot of ($k_{obs} - 18$)/k'' versus $[Cl^-]_e$ is a curve (Fig. 6, bottom). Fitting the data to a curve (using an iterative methodology) gives equation (5), from which the rate law for the reaction of $[Ni(S_2CMe)(triphos)]^+$ with HCl in the presence of Cl^- is derived {equation (6)}; d = 250.0 $dm^3\ mol^{-1}\ s^{-1}$ and e = 18.0 s^{-1}.

$$\frac{k_{obs} - 18}{k''} = \frac{1}{1 + 250[Cl^-]_e} \quad (5)$$

$$\text{Rate} = \frac{a[HCl]_e[Ni(S_2CMe)(triphos)^+] + e}{(1 + b[HCl]_e)(1 + d[Cl^-]_e)} \quad (6)$$

The scatter in the data shown in both plots of Fig. 6 is, we believe, in part, a consequence of the necessary corrections to the concentrations of HCl and Cl^- to allow for the homoconjugation equilibrium {equation (3)}. These corrections use a single value for the homoconjugation equilibrium constant (K_H) over the entire concentration range. It seems likely that the value of K_H might vary slightly with the ionic strength of the solution.

Mechanism. For the R = Et or Bu^n derivatives, the experimental rate law shown in equation (4) is consistent with a mechanism involving two coupled equilibria. Both mechanisms shown in Fig. 7 would give rise to this form of rate law.

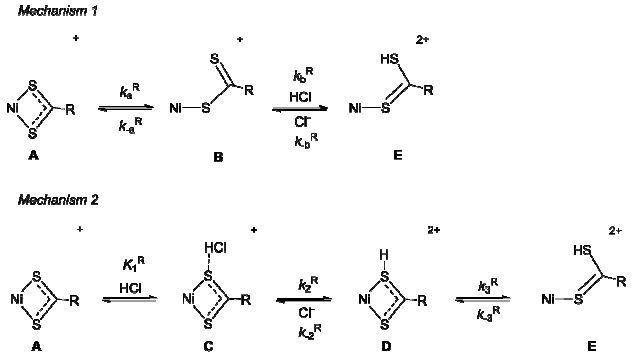

Fig. 7. Mechanisms of protonation of $[Ni(S_2CR)(triphos)]^+$ (R = Me, Et or Bu^n, Ph)

Mechanism 1 involves an initial unimolecular step (possibly ring-opening of the carboxydithioate ligand, k_a^R) which is then protonated in the subsequent step (k_b^R). Assuming that the ring-opened intermediate (**B**) is a steady-state species, the rate law associated with mechanism 1 is that shown in equation (7)

$$\text{Rate} = \frac{\{(k_a^R k_b^R/k_{-a}^R)[HCl]_e + k_{-b}^R[Cl^-]_e\}[Ni(S_2CR)(triphos)^+]}{1 + (k_b^R/k_{-a}^R)[HCl]_e} \quad (7)$$

Although equation (7) is a rate law of the same form as that observed experimentally {equation (4)}, this is not the favoured mechanism for the following reasons. (i) There is no evidence that any $[Ni(S_2CR)(triphos)]^+$ is undergoing rapid chelate ring-opening and closure in the absence of acid. (ii) The inhibiting effect of Cl^- on the reaction between $[Ni(S_2CMe)(triphos)]^+$ and HCl {equation (6)} cannot be explained using this mechanism. (iii) Studies with DCl (*vide infra*) show that both steps in the mechanism are associated with isotope effects, but in mechanism 1, the chelate ring-opening is not dependent on the acid and thus k_a^R can not be associated with an isotope effect.

Mechanism 2 is consistent with the kinetic data for all the complexes described in this paper. The first equilibrium involves hydrogen-bonding of HCl to the complex (to form **C**), whilst the second equilibrium is the intramolecular proton transfer from Cl to S (to form **D**), and the final equilibrium

Table 4. Summary of elementary rate and equilibrium constants for the reactions of $[Ni(S_2CR)(triphos)]^+$ (R = Me, Et, Bu^n or Ph) with mixtures of HCl and Cl^- in MeCN at 25.0 °C.

R	K_1^R / $dm^3\ mol^{-1}$	k_2^R / s^{-1}	$K_1^R k_2^R$ / $dm^3\ mol^{-1}\ s^{-1}$	k_{-2}^R / $dm^3\ mol^{-1}\ s^{-1}$	k_{-2}^R/k_3^R / $dm^3\ mol^{-1}$	k_{-3}^R / s^{-1}	$K_1^R K_2^R$
Me	67	70	4.69×10^3		250	18	
	110[a]	42.5[a]	4.67×10^3 [a]				
Et	84	0.47	39.5	380			0.10
	191[a]	0.26[a]	49.7[a]				
Bu^n	71	0.28	19.9	74			0.27
	83.3[a]	0.21[a]	17.5[a]				
Ph	≤ 6.7	≥ 0.33	2.18	200			0.011

footnote: [a] studies with DCl

corresponds to the chelate ring-opening step (to form **E**). There is nothing unusual about this mechanism for proton transfer. It seems likely that, in general, any proton transfer reaction will involve the formation of a hydrogen-bonded precursor, it is just that in this system (because formation of the hydrogen-bonded precursor is rapid but proton transfer is relatively slow) the precursor accumulates.[5] Similar kinetics have been observed in the protonation reactions of other ligands bound to the robust $\{Ni(triphos)\}^{2+}$ site.[5,7,15]

To accommodate the experimental rate laws for R = Et and Bu^n only the first two equilibria need to be considered (*i.e.* rate-limiting proton transfer). However, to accommodate the experimental rate law for R = Me all three coupled equilibria need to be considered (*i.e.* rate-limiting chelate ring-opening after protonation). The rate law associated with mechanism 2 is derived assuming that formation of the hydrogen-bonded precursor (**C**) from **A** and HCl is a rapidly established equilibrium. The rate law will then depend on whether proton transfer (k_2^R) or the chelate ring-opening (k_3^R) is rate-limiting. If proton transfer is rate limiting (k_2^R is slow and k_3^R is fast) the rate law associated with mechanism 2 is that shown in equation (8). However, if chelate ring-opening is rate-limiting (k_2^R is fast and k_3^R is slow), and **D** is a steady-state intermediate then the rate law for mechanism 2 is that shown in equation (9).

$$\text{Rate} = \frac{\{K_1^R k_2^R[HCl]_e + k_{-2}^R[Cl^-]_e\}[Ni(S_2CR)(triphos)^+]}{1 + K_1^R[HCl]_e} \quad (8)$$

$$\text{Rate} = \{\frac{K_1^R k_2^R[HCl]_e}{(1 + K_1^R[HCl]_e)(1 + \{k_{-2}^R/k_3^R\}[Cl^-]_e)} + k_{-3}^R\}[Ni(S_2CR)(triphos)^+] \quad (9)$$

Equation (8) is the same form as that observed in the reactions with $[Ni(S_2CEt)(triphos)]^+$ and $[Ni(S_2CBu^n)(triphos)]^+$ {equation (4)}, whilst equation (9) is the same form as that observed with $[Ni(S_2CMe)(triphos)]^+$ {equation (6)}. The values of the elementary rate and equilibrium constants for the reactions of $[Ni(S_2CR)(triphos)]^+$ with mixtures of HCl and Cl^- are summarized in Table 4.

It is pertinent to note that for $[Ni(S_2CR)(triphos)]^+$ {R = Et, Bu^n or Ph (*vide infra*)} the observed rate laws only indicate equilibrium protonation of these complexes and, because in these systems proton transfer is rate-limiting, there is no evidence for the subsequent chelate ring-opening step. Nonetheless, we suggest that all the complexes are so similar that the chelate ring-opening follows protonation in all $[Ni(S_2CR)(triphos)]^+$. This proposal is supported by DFT calculations (*vide infra*). Inspection of the data in Table 4 shows that protonation of $[Ni(S_2CMe)(triphos)]^+$ is significantly faster than for the other derivatives. The possible reasons for this will be discussed below. Because protonation is fast for $[Ni(S_2CMe)(triphos)]^+$ the chelate ring-opening step becomes rate-limiting. In contrast, for $[Ni(S_2CEt)(triphos)]^+$ or $[Ni(S_2CBu^n)(triphos)]^+$ proton transfer is slower than chelate ring-opening and hence proton transfer is rate-limiting.

For the equilibrium reaction between $[Ni(S_2CMe)(triphos)]^+$ ($\mathbf{A^{Me}}$) and HCl to form **E** and Cl^-, the overall equilibrium constant can be calculated from the kinetic data presented in Table 4. ($K_1^{Me}.K_2^{Me}.K_3^{Me} = 6.5 \times 10^4$). Using this value we can calculate that in a solution prepared from [$\mathbf{A^{Me}}$] = 1.0 mmol dm^{-3} and [HCl] = 10.0 mmol dm^{-3}, all the nickel complex is converted to $\mathbf{E^{Me}}$. However, we have been unable to isolate $\mathbf{E^{Me}}$ from such reaction mixtures in the absence of Cl^-. In all cases the only Ni-containing product isolated was $[Ni(S_2CR)(triphos)]BPh_4$ (**A**). Furthermore, studies using $^{31}P\{^1H\}$ NMR spectroscopy on solutions containing [$\mathbf{A^{Me}}$] = 1.0 mmol dm^{-3} and [HCl] = 10.0 mmol dm^{-3} showed chemical shifts (associated with the triphos ligand) which were little different from those of $\mathbf{A^{Me}}$ ($\delta \pm 10$ ppm). Similar problems in isolating thiol products in the protonation reactions of Ni-thiolate complexes have been reported for a variety of other systems.[5,7,12,15]

Reaction between $[Ni(S_2CPh)(triphos)]^+$ and HCl in the presence of Cl^-. The kinetics of the reaction between $[Ni(S_2CPh)(triphos)]^+$ and HCl in the presence of Cl^- exhibit a first-order dependence on the concentration of complex. A plot of $k_{obs}/[Cl^-]_e$ versus $[HCl]_e/[Cl^-]_e$ is a straight line with a small intercept as shown in Fig. 8. Thus, the rate law associated with this reaction is shown in equation (10) and is consistent with an equilibrium protonation reaction.

$$\text{Rate} = \{2.18[HCl]_e + 200[Cl^-]_e\}[Ni(S_2CPh)(triphos)^+] \quad (10)$$

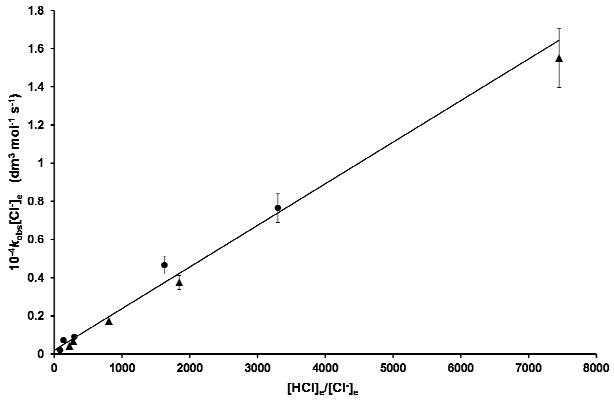

Fig. 8. Kinetic data for the reaction of $Ni(S_2CPh)(triphos)]^+$ (0.5 mmol dm^{-3}) with HCl in the presence of Cl^- in MeCN at 25.0 °C. Graph of $k_{obs}/[Cl^-]_e$ versus $[HCl]_e/[Cl^-]_e$ where subscript e is explained in the text. Data points correspond to: [HCl] = 100.0 mmol dm^{-3}, $[Cl^-]$ = 1.0–15.0 mmol dm^{-3} (●); [HCl] = 150.0 mmol dm^{-3}, $[Cl^-]$ = 1.0–15.0 mmol dm^{-3} (▲). Line drawn is that defined by Equation (10). The error bars correspond to 10% errors.

This rate law is consistent with mechanism 2 and the associated rate law shown in equation (8), where proton transfer is rate-limiting. If $K_1^{Ph}[HCl]_e < 1$, equation (8) simplifies to the rate law shown in equation (11). Comparison of equations (10) and (11) give the values of the elementary rate constants shown in Table 4.

$$\text{Rate} = \{K_1^{Ph}k_2^{Ph}[HCl]_e + k_{-2}^{Ph}[Cl^-]_e\}[Ni(S_2CPh)(triphos)^+] \quad (11)$$

If $K_1^{Ph}[HCl]_e < 1$, we can estimate that $K_1^{Ph} \leq 6.7$ dm^3 mol^{-1}. Comparison of the data in Table 4 shows that proton transfer to $[Ni(S_2CPh)(triphos)]^+$ ($K_1^{Ph}k_2^{Ph}$) is slower than to the alkyl carboxydithioate complexes and this appears to be due, principally, to the lower value of K_1^{Ph} ($k_2^{Ph} \geq 0.33$ s^{-1}). This observation indicates that the basicities of the

carboxydithioate ligands are significantly different when R = aryl compared to when R = alkyl, and that this affects the association between HCl and the complex {*i.e.* formation of the hydrogen-bonded precursor (**C**), K_1^R}, but has less effect on the rates of the intramolecular proton transfer step (k_2^R).

The site of protonation: computational studies. One complication in presenting a rigorous analysis of the kinetics for protonation of $[Ni(S_2CR)(triphos)]^+$ is that there are two distinct sulfur sites in the complex. X-ray crystallography reveals a trigonal bipyramidal structure for all $[Ni(S_2CR)(triphos)]^+$, in which one sulfur of the carboxydithioate ligand sits in the equatorial plane while the other occupies an axial position (Figs. 2 and 3). The kinetics described above cannot distinguish between a mechanism involving protonation of a single sulfur site or two parallel pathways, each associated with protonation of a different sulfur. Using molecular mechanics calculations (GAUSSIAN03 package,[16] geometries optimized at the B3LYP/Lanl2dz levels of theory and including solvent, see ESI) we have explored the protonation of each sulfur in $[Ni(S_2CR)(triphos)]^+$ (R = Me or Ph). The calculations indicate, for both R = Me and Ph, that protonation of the equatorial sulfur (S_2) results in chelate ring-opening to form species $\mathbf{E}^{\mathbf{R}}$, with a pendant S_2H group (Fig. 9). Selected calculated bond lengths and bond angles for R = Ph are shown in Table 5 and the analogous data for R = Me, together with pictures of $\mathbf{E}^{\mathbf{R}}$, are shown in ESI. The calculated bond angles for $\mathbf{E}^{\mathbf{R}}$ indicate that the Ni has a square-planar geometry (Table 5 and ESI). This result is in line with the interpretation of the kinetics {equations (8) and (9)}. Interestingly, calculations indicate that protonation of the axial sulfur (S_1) in $[Ni(S_2CR)(triphos)]^+$ can also occur but is associated with only relatively minor changes in the structure

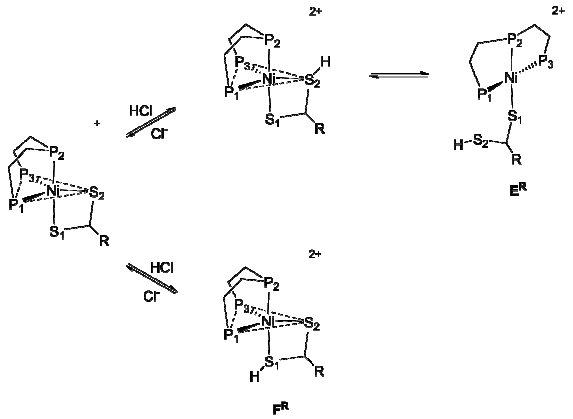

Fig 9. Consequences of protonation at axial (S_1) and equatorial (S_2) sulfur of $[Ni(S_2CR)(triphos)]^+$ (R = Me or Ph).

and no chelate ring-opening. Comparison of the selected calculated bond lengths and bond angles for $\mathbf{E}^{\mathbf{Ph}}$ and $\mathbf{F}^{\mathbf{Ph}}$ (Table 5) and the analogous dimensions for $[Ni(S_2CPh)(triphos)]^+$ from the X-ray crystallographic data (Table 3) demonstrate the major dimension changes involved when protonation occurs at S_2, but the relatively minor changes associated with protonation at S_1.

It seems likely that chelate ring-opening occurs after protonation of S_2 because reorganization to the square-planar geometry is energetically rather undemanding, requiring only a slight opening up of the P_1–Ni–P_3 angle. In contrast, it seems likely that the reorganization to a square-planar geometry after protonation at S_1 and cleavage of the Ni–S_1 bond is energetically more demanding since it requires opening up of the P_1–Ni–P_3 angle and movement of the Ni–S_2 bond.

In the light of the results from these calculations we need to consider a modification to the mechanism in Fig. 7 to accommodate the protonation of both sulfur sites and the different geometrical changes which accompany the protonations (Fig. 10). Assuming that the rates of proton transfer to both S_1 and S_2 are slow and that the mechanism for protonation of both sites is the same, the modified mechanism is associated with the rate law shown in equation (12). Comparison of equation (8) (single site protonation) and equation (12) yields the relationships shown in equations (13) – (15).

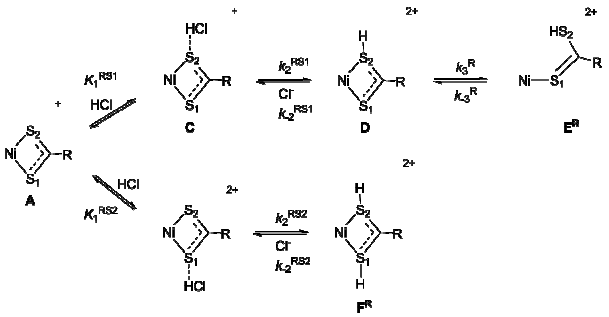

Fig. 10. Mechanism for the reactions of $[Ni(S_2CR)(triphos)]^+$ with HCl in the presence of Cl^-, accomodating the results of the DFT calculations which indicate that protonation can occur at both sulfurs but with different structural consequences .

$$\text{Rate} = \frac{\{(K_1^{RS1}k_2^{RS1} + K_1^{RS2}k_2^{RS2})[HCl]_e}{1 + (K_1^{RS1} + K_1^{RS2})[HCl]_e} + (k_{-2}^{RS1} + k_{-2}^{RS2})[Cl^-]_e\}[Ni(S_2CR)(triphos)^+] \quad (12)$$

$$K_1^R = K_1^{RS1} + K_1^{RS2} \quad (13)$$

$$k_2^R = \frac{K_1^{RS1}k_2^{RS1} + K_1^{RS2}k_2^{RS2}}{K_1^{RS1} + K_1^{RS2}} \quad (14)$$

$$k_{-2}^R = k_{-2}^{RS1} + k_{-2}^{RS2} \quad (15)$$

Although the results from the DFT calculations indicate both S_1 and S_2 can be protonated (but chelate ring-opening is only associated with protonation of S_2), the calculations give no insight into the relative rates of each pathway. For example, protonation at S_2 could be much faster than at S_1, in which case the simpler rate law {equation (8)} associated with a single-site protonation mechanism is applicable. However if the rates of protonation of S_1 and S_2 are similar then equation (12) is the accurate description of the kinetics. For simplicity, in the remainder of the discussion, the results will be interpreted in terms of a single-site protonation {Fig. 7 and equation (8)} but where the interpretation would be compromised if a two-site protonation model is more applicable {Fig. 10 and equation (12)} the issues will be discussed.

Table 5. Selected bond lengths and bond angles of $Ni(S(SH)CPh)(triphos)]^{2+}$ from DFT calculations

	Complex $\mathbf{E}^{Ph}$	Complex $\mathbf{F}^{Ph}$
bond lengths		
Ni–P_1	2.2665	2.2665
Ni–P_2	2.2176	2.2630
Ni–P_3	2.2630	2.2176
Ni–S_1	2.2865	2.0423
Ni–S_2	3.5122	2.4400
bond angles		
P_1–Ni–P_2	85.90	85.90
P_1–Ni–P_3	152.31	152.31
P_1–Ni–S_1	94.17	90.91
P_1–Ni–S_2		104.47
P_2–Ni–P_3	85.25	85.25
P_2–Ni–S_1	179.93	167.33
P_2–Ni–S_2		123.24
P_3–Ni–S_1	94.69	92.04
P_3–Ni–S_2		102.33

Isotope effects for reactions of $[Ni(S_2CR)(triphos)]^+$ (R = Me, Et or Bu^n) with HCl. Because proton transfer from HCl to $[Ni(S_2CR)(triphos)]^+$ in MeCN is slow (and rate-limiting for R = Et, Bu^n or Ph) these reactions would be expected to be associated with a kinetic isotope effect when HCl is replaced by DCl.[16] Furthermore, proton transfer to $[Ni(S_2CR)(triphos)]^+$ (R = Me, Et or Bu^n) involves initial formation of the hydrogen-bonded species (K_1^R) followed by intramolecular proton transfer (k_2^R) and these steps are distinguishable in the analysis of the kinetics. Thus, measuring the kinetics of the reactions of DCl with $[Ni(S_2CR)(triphos)]^+$ allow us to determine how the isotopic change in the acid affects both K_1^R and k_2^R.

In principle, we could also measure the isotope effect for the reaction between DCl and $[Ni(S_2CPh)(triphos)]^+$. However, there is a problem with analysing the kinetic data in this case. As outlined earlier, mixtures of HCl and Cl^- are involved in the homoconjugation equilibrium reaction shown in Equation (3) and the concentrations of $[HCl]_e$ and $[Cl^-]_e$ in such mixtures can be calculated using the literature homoconjugation equilibrium constant (K_H). Unfortunately, the homoconjugation equilibrium constant for mixtures of DCl and Cl^- is unknown, and would be expected to be different from K_H. Thus, in mixtures containing DCl and Cl^-, the concentrations of $[DCl]_e$ and $[Cl^-]_e$ cannot be calculated. The same problem is encountered in attempting to measure the isotope effect for the reaction between DCl and $[Ni(S_2CR)(triphos)]^+$ (R = Me, Et or Bu^n) in the presence of Cl^-. Consequently, we have only measured the kinetics of the reactions of $[Ni(S_2CR)(triphos)]^+$ (R = Me, Et or Bu^n) with DCl in the absence of Cl^-.

The kinetics of the reactions between $[Ni(S_2CR)(triphos)]^+$ (R = Me, Et or Bu^n) and DCl in MeCN follow the same general behaviour as the analogous reactions with HCl (Fig. 5); the reactions exhibit a first-order dependence on the concentration of complex and a non-linear dependence on the concentration of DCl. Analysis of the dependence of the reaction rate on the concentration of DCl (using plots of $1/k_{obs}$ versus 1/[DCl]), yields the values of $(K_1^R)^D$ and $(k_2^R)^D$ shown in Table 4. The data show that the overall isotope effect for transfer of the proton from acid to $[Ni(S_2CR)(triphos)]^+$ $\{(K_1^R k_2^R)^H/(K_1^R k_2^R)^D\}$ is small for all complexes and varies from an apparent inverse to a normal isotope effect (0.79–1.14). Inspection of the individual isotope effects for K_1^R and k_2^R reveals that the small isotope effects for $(K_1^R k_2^R)^H/(K_1^R k_2^R)^D$ are a consequence of larger, but opposing, isotope effects for the individual $(K_1^R)^H/(K_1^R)^D$ and $(k_2^R)^H/(k_2^R)^D$. Thus, for all complexes, the formation of the hydrogen-bonded species $\{[Ni(S_2CR)(triphos)]\ldots HCl\}^+$ (**C**) is associated with an inverse equilibrium isotope effect $\{(K_1^R)^H/(K_1^R)^D = 0.44–0.85\}$ and the intramolecular proton transfer step is associated with a normal primary isotope effect $\{(k_2^R)^H/(k_2^R)^D = 1.33–1.81\}$. It is to be anticipated that DCl will be a slightly stronger acid than HCl in MeCN and this is reflected in the values of $(K_1^R)^H/(K_1^R)^D$ (< 1.0). The normal kinetic isotope effects for $(k_2^R)^H/(k_2^R)^D$ (> 1.0) are consistent with this step involving the intramolecular transfer of a proton.[17]

The rates of protonation of $[Ni(S_2CR)(triphos)]^+$. The studies presented herein show that the rates of proton transfer to coordinated carboxydithioate in $[Ni(S_2CR)(triphos)]^+$ (R = Me, Et, Bu^n or Ph), and deprotonation of the corresponding coordinated conjugate acid, are significantly slower than the diffusion-controlled limit. At least in part this is because the reactions are thermodynamically unfavourable {*e.g.* $(pK_a^{HCl} - pK_a^{PhCS2H}) = 2.0$ (*vide infra*)}.[18] The kinetic analyses presented above allow us to calculate the rate constants for the intramolecular proton transfer step (k_2^R) within the hydrogen-bonded intermediate (**C**; R = Et, Bu^n or Ph). The results in Table 4 show that the values of k_2^R are essentially independent of R. It is also evident from the data in Table 4 that the protonation of $[Ni(S_2CMe)(triphos)]^+$ is appreciably faster than that of $[Ni(S_2CEt)(triphos)]^+$ or $[Ni(S_2CBu^n)(triphos)]^+$ ($K_1^{Me}k_2^{Me} : K_1^{Et}k_2^{Et} : K_1^{Bu}k_2^{Bu} = 236 : 2 : 1$). The reason for the increased reactivity of $[Ni(S_2CMe)(triphos)]^+$ is not clear. The difference in rates seems too large to be attributed to an electronic effect of the R group modulating the basicity of sulfur; after all, the pK_as of $MeCO_2H$, $EtCO_2H$ and Bu^nCO_2H are all the same {pK_a (in water) = 4.79±0.01}.[19] It seems more likely that the difference in rates is a consequence of the size of the R = alkyl substituents. Inspection of the values of K_1^R and k_2^R shows that $K_1^R = 76±9$ dm^3 mol^{-1}, essentially independent of the R substituent. The difference in the rates is because the rate of intramolecular proton transfer for the R = Me derivative is *at least* 150 times faster than for the other R = alkyl derivatives. This suggests that the larger R substituents interfere with HCl hydrogen bonding to $[Ni(S_2CR)(triphos)]^+$ (in **C**), and attaining the optimal geometry for proton transfer. An alternative possible explanation is that the significant difference in the rates of protonation of $[Ni(S_2CMe)(triphos)]^+$ and the other derivatives is a consequence of a change in the dominant site of protonation (S_1 or S_2).

The basicities of $[Ni(S_2CR)(triphos)]^+$. In principle, the elementary rate and equilibrium constants determined from analysis of the kinetics of the reactions of $[Ni(S_2CR)(triphos)]^+$ (R = Et, Bu^n or Ph) with mixtures of HCl and Cl^- allow calculation of the pK_a^R of the coordinated carboxydithioic acids.

The equilibrium constant for the protonation of $[Ni(S_2CR)(triphos)]^+$ in the single site model is $K_1^R K_2^R = K_1^R k_2^R/k_{-2}^R$. These values are presented in Table 4. Using the literature pK_a of HCl in MeCN (8.9),[20] and the value of $K_1^R K_2^R$,

the pK_a^R of $[Ni(S_2CR)(triphos)]^+$ in MeCN can be calculated: $pK_a^{Et} = 7.9$; $pK_a^{Bu} = 8.3$; $pK_a^{Ph} = 6.9$. The notable feature is that pK_a^R is rather insensitive to the R-substituent. Similar levelling effects for acidities of ligands have been noted before.[7,21] As expected, the R = Ph derivative is slightly more acidic than the R = alkyl derivatives. The different kinetics for the reaction of $[Ni(S_2CMe)(triphos)]^+$ with mixtures of HCl and Cl^- means that $K_1^{Me}K_2^{Me}$, and hence pK_a^{Me}, cannot be calculated.

The pK_a^R values indicate that these carboxydithioic acid ligands (when bound to the $\{Ni(triphos)\}^{2+}$ site) are significantly more acidic than the free acids (in MeCN: $EtCS_2H$, $pK_a = 13.4$; $PhCS_2H$, $pK_a = 13.2$).[19,22] Thus, coordination of the carboxydithioic acid results in an increase in the acidity $\{\Delta(pK_a - pK_a^{Et}) = 5.5; \Delta(pK_a - pK_a^{Ph}) = 6.3\}$. Interestingly, a similar effect has been observed with PhSH coordinated to the $\{Ni(triphos)\}^{2+}$ site $\{\Delta(pK_a - pK_a^{PhSH}) = 5.4\}$.[5]

These calculations need to be treated with considerable caution for two reasons. First, the pK_as have been calculated from kinetic data where proton transfer is slow. Previous studies have indicated that proton transfer reactions with $lutH^+$ to $[Ni(XPh)(triphos)]^+$ are slow, at least in part, because steric interactions of the bulky phenyl substituents on triphos interfere with the approach of the sterically demanding $lutH^+$ towards the basic ligand.[7] We have suggested that calculating the pK_a of the coordinated PhXH, in these cases, does not correspond to the true basicity of the ligand, but rather reflects the rates of proton transfer to and from the PhX ligand. Clearly, HCl is much less sterically demanding than $lutH^+$ and this, together with the less sterically demanding 5-coordinate $[Ni(S_2CR)(triphos)]^+$, suggests that the values of pK_a^R determined from the kinetics described in this paper are more likely to reflect the true acidity of the coordinated carboxydithioic acid. Secondly, if we consider the entirely general mechanism involving a two-site protonation model (Fig. 10), then the associated rate law is equation (12). In this case the pK_as calculated from the kinetic data would be meaningful only if one pathway dominates (*e.g.* $K_1^{RS1}k_2^{RS1} > K_1^{RS2}k_2^{RS2}$ and $k_{-2}^{RS1} > k_{-2}^{RS2}$), or if both pathways occur at the same rate (*i.e.* $K_1^{RS1}k_2^{RS1} \sim K_1^{RS2}k_2^{RS2}$ and $k_{-2}^{RS1} \sim k_{-2}^{RS2}$).

Conclusions

The studies reported herein show that the rates of protonation of coordinated carboxydithioates are significantly slower than the diffusion-controlled limit ($k_{diff} \sim 3.7 \times 10^{10}$ dm^3 mol^{-1} s^{-1} in MeCN)[23]. The reason for this slowness is, in part, because the reactions are thermodynamically unfavourable. However, the rates of proton transfer are *ca* 10^7–10^{10} slower than the diffusion-controlled limit and the thermodynamic argument cannot account for this large difference. It seems likely, as suggested earlier for the protonation reactions of $[Ni(XPh)(triphos)]^+$ (X = O, S or Se), that steric factors contribute to the slowness of the reactions.[7]

The kinetics for the protonation of $[Ni(S_2CR)(triphos)]^+$ (R = alkyl) with HCl indicate a two-step equilibrium mechanism. The initial step involves the rapid formation of a hydrogen-bonded precursor (K_1^R) and this is followed by intramolecular proton transfer (k_2^R). It seems likely that for all $[Ni(S_2CR)(triphos)]^+$ (R = alkyl or aryl) the same mechanism operates but only when R = alkyl does the precursor accumulate to concentrations sufficient to perturb the kinetics. The measured kinetic isotope effects for the complete transfer of a proton from HCl to $[Ni(S_2CR)(triphos)]^+$ (R = Me, Et or Bu^n) are small $\{(K_1^Rk_2^R)^H/(K_1^Rk_2^R)^D = 0.79–1.14\}$. This is the result of a small inverse equilibrium isotope effect for the formation of the precursor hydrogen-bonded adduct $\{(K_1^R)^H/(K_1^R)^D = 0.44–0.85\}$ and a significant kinetic primary isotope effect for the intramolecular proton transfer step $\{(k_2^R)^H/(k_2^R)^D = 1.33–1.81\}$. Finally, DFT calculations indicate that protonation can occur at either the equatorial or the axial sulfur sites, but that chelate ring-opening of the carboxydithionic acid occurs only after protonation of the equatorial sulfur. The ways in which parallel protonation of the two sulfur sites would complicate the analyses and interpretation of the kinetics have been discussed.

Acknowledgements

The authors acknowledge the use of the EPSRC UK National Service for Computational Chemistry Software (NSCCS) at Imperial College London in carrying out this work. A.A. thanks the Iraqi Ministry of Higher Education and Scientific Research for a studentship. Crystallographic studies were part-funded by an EPSRC equipment grant, facilitated by access to equipment at Durham University Chemistry Department for one of the structures during refurbishment at Newcastle, and made possible for two of the compounds by access granted to beamline I19 at Diamond Light Source, for which we are very grateful.

Notes and references

[a] School of Chemistry, Newcastle University, Newcastle upon Tyne, NE1 7RU, UK; [b] Department of Chemistry, College of Science, University of Basrah, Basrah, Iraq.

† Electronic Supplementary Information (ESI) available: [summary of kinetic data for the reactions of $[Ni(S_2CR)(triphos)]^+$ (R = Me, Et, Bu^n or Ph) with HCl or mixtures of HCl and Cl^- in MeCN, crystallography data, selected bond lengths and angles, together with pictures of optimized calculated structures for protonated complexes]. See DOI: 10.1039/b000000x/

1 (a) K. W. Kramarz and J. R. Norton, *Prog. Inorg. Chem.*, 1994, **42**, 1, and refs therein; (b) R. A. Henderson, *Angew. Chemie, Int. Ed.*, 1996, **35**, 946, and refs therein.

2 (a) M. Eigen, *Angew. Chemie, Int. Ed.,* 1964, **3**, 1; (b) M. M. Kreevoy, D. S. Sappenfield and W. Schwabacher, *J. Phys. Chem.*, 1965, **69**, 2287.

3 (a) C. F. Bernasconi and R. L. Montanez, *J. Org. Chem*. 1997, **62**, 8162; (b) C. F. Bernasconi, D. M. Weirsema, W. Stronach, *J. Org. Chem*., 1993, **58**, 217, and refs therein.

4 (a) R. H. Holm, P. Kennepohl and E. I. Solomon, *Chem. Rev.* 1996, **96**, 2239; (b) S. C. Lee and R. H. Holm, *Chem. Rev*. 2004, **104**, 1135; (c) D. W. Mulder, M. W. Ratzloff, E. M. Shepard, A. S. Byer, S. M. Noone, J. W. Peters, J. B. Broderick, and P. W. King, *J. Am. Chem. Soc*., 2013, **135**, 6921; (d) B. M. Hoffman, D. Lukoyanov, Z.-Y. Yang, D. R. Dean, and L. C. Seefeldt, *Chem. Rev*., 2014, **114**, 4041; (e) A. Jablonskyte, L. R. Webster, T. R. Simmons, J. A. Wright and C. J. Pickett, *J. Am. Chem. Soc*., 2014, **136**, 13038.

5 V. Autissier, P. M. Zarza, A. Petrou, R. A. Henderson, R. W. Harrington, W. Clegg, *Inorg. Chem.,* 2004, **43**, 3106.

6 C. Cauquis, A. Deronzier, D. Serve and E. Vieil, *J. Electroanal. Chem. Interfacial Electrochem*., 1975, **60**, 205.

7 A. Alwaaly and R. A. Henderson, *Chem Commun.*, 2014, **50**, 9669.

8 W. Clegg and R. A. Henderson, *Inorg. Chem.*, 2002, **41**, 1128.

9 C. Bonnans-Plaisance and J.-C. Gressiw, *J. Chem. Ed.,* 1988, **65**, 93, and refs therein.

10 (a) CrysAlisPro software, Agilent Technologies Ltd., Oxford, UK, 2013. (b) APEX2, SADABS and SHELXTL, Bruker AXS Inc., Madison, Wisconsin, USA, 2014. (c) CrystalClear, Rigaku Corp., Tokyo, Japan, 2013. (d) SHELXL-2014, G. M. Sheldrick, University of Göttingen, Germany, 2014. (e) OLEX2, O. V. Dolomanov, L. J. Bourhis, R. J. Gildea, J. A. K. Howard and H. Puschmann, *J. Appl. Crystallogr*. 2009, **42**, 339.

11 W. Addison, T. Nageswara Rao, J. Reedijk, J. van Rijn and G. C. Verschoor, *J. Chem. Soc., Dalton Trans*., 1984, 1349. This paper defines the angular structural parameter, $\tau = (\beta - \alpha)/60$ (where α = smaller of basal angles and β = larger of basal angles). The parameter τ is an index of trigonality in 5-coordinate complexes. For a perfect square-based pyramid, $\tau = 0$ and for a perfect trigonal bipyramid $\tau = 1.0$. For the complexes described herein $\beta = P_2NiS_1$ and $\alpha = P_1NiS_2$. Hence, R = Et, $\tau = 0.84$; R = Ph, $\tau = 1.15$; R = C_6H_4OMe-4, $\tau = 1.01$; R = C_6H_4Cl-4, $\tau = 0.96$.

12 A. Petrou, A. D. Koutselos, H. S. Wahab, W. Clegg, R. W. Harrington and R. A. Henderson, *Inorg. Chem*., 2011, **50**, 847.

13 R. G. Wilkins, *Kinetics and Mechanisms of Reactions of Transition Metal Complexes*, VCH, Weinheim, 2nd edition, 1991, p 24.

14 J. F. Coetzee, *Prog. Phys. Org. Chem*., 1967, **4**, 45.

15 V. Autissier, W. Clegg, R. W. Harrington and R. A. Henderson, *Inorg. Chem.,* 2004, **43**, 3098.

16 M. J. Frisch *et al., Gaussian 03, revision D.01*, Gaussian, Inc., Wallingford, CT, 2004.

17 (a) S. E. Scheppele, *Chem. Rev*., 1972, **72**, 511, and refs therein; (b) G. Parkin and J. E. Bercaw, *Organometallics*, 1989, **8**, 1172.

18 R. P. Bell, *The Proton in Chemistry* (2nd edition), Chapman and Hall, London, 1973, ch 11.

19 Advanced Chemistry Development (ACD/Labs) Software V11.02 (© 1994-2014 ACD/Labs).

20 K. Izutsu, *Acid-Base Dissociation Constants in Dipolar Aprotic Solvents*; Blackwell Scientific: Oxford, UK, 1990.

21 B. L. Westcott, N. E. Gruhn and J. H. Enemark, *J. Am. Chem. Soc*., 1998, **120**, 3382.

22 Calculated pK_a (in water) from reference 19 then correcting to the pK_a in MeCN using equations in, B. G. Cox, *Acids and Bases Solvent Effects on Acid-Base Strength*, Oxford University Press, UK, 2013.

23 F. Wilkinson, A. F. Olea, D. J. McGarvey and D. R. Worrall, *J. Braz. Chem. Soc*., 1995, **6**, 211–220.

Mechanisms and rates of proton transfer to coordinated carboxydithioates: studies on $[Ni(S_2CR)\{PhP(CH_2CH_2PPh_2)_2\}]^+$ (R = Me, Et, Bu^n or Ph)

Ahmed Alwaaly, William Clegg, Richard A. Henderson*, Michael R. Probert and Paul G. Waddell

ABSTRACTS

Graphical Abstract

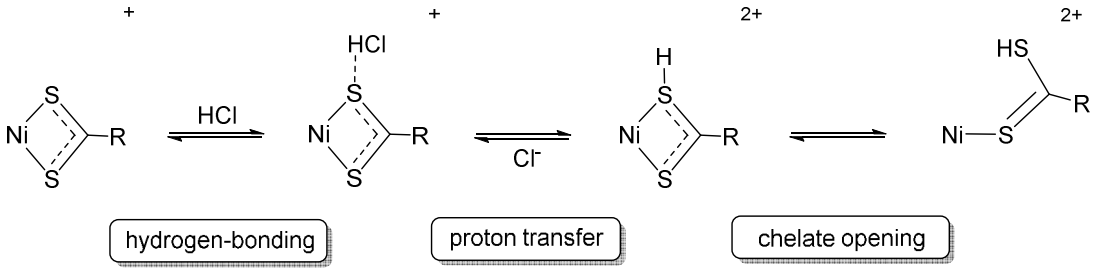

Textual Abstract

Kinetics of protonation of $[Ni(S_2CR)(PhP\{CH_2CH_2PPh_2\}_2)]^+$ (R = Me, Et, Bu^n or Ph) with HCl reveals hydrogen-bonded precursor and subsequent chelate opening.